

**PHOTOCATALYTIC PERFORMANCE OF F-
GNP/ZnO COMPOSITE FOR METHYLENE
BLUE DEGRADATION UNDER UV-VIS LIGHT
IRRADIATION**

RABIATUL ALIAH BINTI MAHMUD

UNIVERSITI SAINS MALAYSIA

2020

**PHOTOCATALYTIC PERFORMANCE OF F-
GNP/ZnO COMPOSITE FOR METHYLENE
BLUE DEGRADATION UNDER UV-VIS
LIGHT IRRADIATION**

by

RABIATUL ALIAH BINTI MAHMUD

**Thesis submitted in fulfilment of the requirements
for the degree of
Master of Science**

August 2020

ACKNOWLEDGEMENT

This master thesis was completed with the guidance and help from several individuals who somehow or another contributed and spending their valuable time in completing this work.

Foremost, I would like to express my sincere gratitude to my research supervisor, Prof. Dato' Ir Dr. Abdul Rahman bin Mohamed for giving me opportunity and providing invaluable guidance throughout the research. The ultimate support in all ways were highly appreciated for making my journey easier in completing my study.

In addition, I sincerely thanks to Dr. Khozema bin Ahmed Ali and Dr. Lutfi Kurnianditia Putri for the guidance and encouragement throughout my study. Thanks for the invaluable time and assistance in sharing knowledge and giving insightful comments.

I am grateful acknowledging Long-Term Research Grant Scheme (LRGS, 203/PJKIMIA/6720009) for providing me financial support in my Master study.

I would like to express my deep and sincere gratitude to my friends, Anis Natasha binti Shafawi, Zaza Hazrina binti Hashim, Noor Izzati binti Md Rosli and Rabita binti Firdaus for the moments we shared along the studying journey. Thanks for the support and precious ideas for me to complete this program.

This work is dedicated to my parents Mahmud bin Mohamed Mustapha and Hasimah binti Mansor, for their uncountable sacrifices and moral support in completing this master program. I am extremely grateful to my sisters and brothers, Nurul Hidayah, Nurul Nadiah, Fathimahtul Zahra, Siti Zaleha, Ahmad Yusri and Sharil Anuar for endless moral and financial supports during my studying journey.

TABLE OF CONTENTS

ACKNOWLEDGEMENT.....	ii
TABLE OF CONTENTS.....	iii
LIST OF TABLES.....	ix
LIST OF FIGURES.....	xi
LIST OF ABBREVIATIONS.....	xiv
LIST OF SYMBOLS.....	xvi
ABSTRAK.....	xvii
ABSTRACT.....	xix
CHAPTER 1 – INTRODUCTION.....	1
1.1 Wastewater Crisis.....	1
1.2 Organic Pollutant.....	3
1.3 Conventional Wastewater Remediation.....	7
1.4 Advance Oxidation Processes (AOPs).....	8
1.5 Semiconductor Photocatalysts.....	9
1.6 Problem Statement.....	10
1.7 Research Objectives.....	12

1.8	Scope of Study.....	13
1.9	Thesis Organization.....	14
CHAPTER 2 – LITERATURE REVIEW.....		16
2.1	Properties and Application of MB.....	16
2.2	Photocatalysis.....	17
2.3	ZnO in Photocatalysis Process.....	22
	2.3.1 Modification of ZnO catalyst.....	25
2.4	Graphene in Photocatalysis.....	28
2.5	Graphene/ZnO Heterostructure in MB Degradation.....	37
2.6	Catalyst Preparation.....	38
2.7	Adsorption Kinetic Study.....	40
2.8	Photocatalysis Kinetic Study.....	44
2.9	Process Operating Parameter Study.....	45
	2.9.1 Catalyst loading.....	45
	2.9.2 Initial pollutant concentration.....	47
	2.9.3 pH of solution.....	48
2.10	Summary.....	50

CHAPTER 3 – MATERIALS AND METHOD.....	51
3.1 Materials and Chemicals.....	51
3.2 Photocatalyst Preparation.....	53
3.3 Characterization of F-GNP/ZnO Composites.....	54
3.3.1 X-ray diffraction (XRD).....	55
3.3.2 Scanning electron microscopy (SEM).....	55
3.3.3 High-resolution transmission electron microscopy (HRTEM).....	55
3.3.4 Energy dispersive x-ray (EDX).....	56
3.3.5 Atomic absorption spectroscopy (AAS).....	56
3.3.6 Fourier transform infrared spectroscopy (FTIR).....	56
3.3.7 Raman spectroscopy.....	57
3.3.8 Surface area analysis.....	57
3.3.9 UV-vis diffuse reflectance spectroscopy (UV-vis DRS).....	57
3.3.10 Photoluminescence (PL).....	58
3.4 Photocatalytic Batch Reactor.....	58
3.5 Adsorption and Photocatalytic Degradation of MB.....	59
3.6 Adsorption and Degradation Kinetic Models.....	60

3.7	Scavenger Test.....	60
3.8	Process Parameter Studies.....	61
CHAPTER 4 – RESULTS AND DISCUSSION.....		63
4.1	Effect of GNP Loading on Catalyst Preparation.....	63
4.1.1	Catalyst characterization.....	63
4.1.1 (a)	X-ray diffraction (XRD).....	64
4.1.1 (b)	Scanning electron microscopy (SEM).....	67
4.1.1 (c)	High-resolution transmission electron microscopy (HRTEM).....	70
4.1.1 (d)	Energy dispersive x-ray (EDX).....	72
4.1.1 (e)	Atomic absorption spectroscopy (AAS).....	73
4.1.1 (f)	Fourier transform infrared spectroscopy (FTIR).....	74
4.1.1 (g)	Raman spectroscopy.....	76
4.1.1 (h)	Surface area analysis.....	78
4.1.1 (i)	UV-vis diffuse reflectance spectroscopy (UV-vis DRS).....	83

4.1.1 (j)	Photoluminescence (PL).....	85
4.1.2	Effect of GNP loading in F-GNP/ZnO composites on MB removal.....	87
4.1.2 (a)	Adsorption of MB and kinetic study.....	87
4.1.2 (b)	Photodegradation of MB and kinetic study.....	92
4.2	Comparison in MB Degradation by Graphene-ZnO Catalyst.....	97
4.3	Robustness of F-GNP/ZnO Catalyst.....	99
4.4	Photocatalysis Operating Parameter.....	101
4.4.1	Effect of catalyst loading.....	101
4.4.2	Effect of initial MB concentration.....	103
4.4.3	Effect of pH solution.....	104
4.5	Photocatalytic Mechanisms.....	108
CHAPTER 5 – CONCLUSIONS AND RECOMMENDATIONS.....		112
5.1	Conclusions.....	112
5.2	Recommendations.....	114

REFERENCES..... 115

APPENDICES 130

LIST OF PUBLICATION 131

LIST OF TABLES

	Page
Table 1.1 Classification of dyes based on the chromophores and auxochromes groups (Berradi <i>et al.</i> , 2019).	5
Table 1.2 Classification of dyes based on the auxochromes groups (Rahman, 2016).	6
Table 2.1 Properties of MB (Hadi <i>et al.</i> , 2015; Qiao <i>et al.</i> , 2016).	17
Table 2.2 Comparative oxidizing power of different oxidants (Teoh <i>et al.</i> , 2012).	21
Table 2.3 Properties of ZnO semiconductor (Henni <i>et al.</i> , 2019; Peter <i>et al.</i> , 2018).	22
Table 2.4 Modifications of ZnO from previous studies.	29
Table 2.5 Summary of the catalyst preparation method, the organic pollutant degraded, the light source used and results for graphene/ZnO composites.	41
Table 2.6 Different kinetic model and its respective function (Çırak <i>et al.</i> , 2019; Firdaus <i>et al.</i> , 2019; Md Rosli <i>et al.</i> , 2018).	45
Table 2.7 Effect of catalyst loading on degradation efficiency.	46
Table 2.8 Effect of initial pollutant concentration on degradation efficiency.	47
Table 2.9 Effect of pH solution on degradation efficiency.	49
Table 3.1 List of chemicals and reagents.	53
Table 3.2 List of chemical scavengers and its radicals' species.	61
Table 3.3 Process operating parameters for 45% F-GNP/ZnO composite.	61

Table 4.1	Average crystallite size for pure ZnO n.p and F-GNP/ZnO composites.	66
Table 4.2	Elemental composition of Zn, C and O determined using EDX analysis.	73
Table 4.3	Elemental composition of and Zn using AAS.	74
Table 4.4	Textural properties for photocatalysts.	80
Table 4.5	Adsorption parameters and kinetics for different weight percentage of GNP in the composites.	89
Table 4.6	Photocatalytic parameters and kinetics for different weight percentage of GNP in the F-GNP/ZnO composites.	94
Table 4.7	Comparison of Graphene-ZnO composites performance in MB degradation depending on the light source, reaction time and photocatalyst preparation.	98
Table 4.8	AAS and BET analysis of 45% F-GNP/ZnO composite before and after MB removal.	100
Table 4.9	Zeta potential value of 45% F-GNP/ZnO composite in different pH dye solution.	105

LIST OF FIGURES

		Page
Figure 1.1	The percentage of (a) water in Earth resources, (b) fresh water among the Earth's water and (c) the available water to be used (Wecker, 2017).	2
Figure 1.2	Statistical of different pollutions in Malaysia (Mei <i>et al.</i> , 2016).	3
Figure 2.1	Schematic diagram of heterogeneous catalyst mechanism (Moniz <i>et al.</i> , 2015).	18
Figure 2.2	Crystal structure of ZnO (a) cubic rocksalt, (b) cubic zinc blende and (c) hexagonal wurtzite ZnO. Shaded grey and black circles denoted as Zn and O atoms, respectively (Morkoç & Özgür, 2008).	23
Figure 2.3	Band gap position of different semiconductors (Ma <i>et al.</i> , 2017).	24
Figure 3.1	Flow chart for method study in this research.	52
Figure 3.2	Process flow chart for F-GNP/ZnO composites preparation.	54
Figure 3.3	Schematic diagram of batch reactor experimental setup.	59
Figure 4.1	XRD patterns for pure ZnO n.p, 15%, 45% and 60% F-GNP/ZnO composites.	65
Figure 4.2	SEM images for (a and b) pure ZnO n.p, (c and d) 15% F-GNP/ZnO, (e and f) 45% F-GNP/ZnO, and (g and h) 60% F-GNP/ZnO composites.	68
Figure 4.3	Particle size distributions obtained from SEM analysis for (a) pure ZnO n.p and (b) 45% F-GNP/ZnO composite.	69

Figure 4.4	HRTEM images of 45% F-GNP/ZnO composite with (a) low magnification and (b) high magnification (arrow indicates ZnO n.p).	71
Figure 4.5	EDX spectrum for (a) pure ZnO n.p, (b) 15% F-GNP/ZnO, (c) 45% F-GNP/ZnO and (d) 60% F-GNP/ZnO composites.	72
Figure 4.6	FTIR spectrum of GNP, F-GNP, pure ZnO n.p, and F-GNP/ZnO composites with different weight percentage of GNP.	75
Figure 4.7	Raman spectrum of pure ZnO n.p, GNP, F-GNP and F-GNP/ZnO composites.	77
Figure 4.8	N ₂ adsorption-desorption analysis of different weight percentage of GNP in the F-GNP/ZnO composite.	79
Figure 4.9	BJH pore size distributions which describe the concentrations of pores of various of sizes.	81
Figure 4.10	BJH pore size distributions which describe the pore volumes over any ranges of pore sizes.	82
Figure 4.11	UV-vis DRS spectra of pure ZnO n.p and F-GNP/ZnO composites.	84
Figure 4.12	Enlarged view of absorption edge in UV-vis DRS spectra within the wavelength of 300 – 450 nm.	85
Figure 4.13	PL analysis for pure ZnO n.p and F-GNP/ZnO composites.	86
Figure 4.14	Influence of graphene weight percentage on MB adsorption.	88
Figure 4.15	Pseudo-second-order model for MB removal with different weight percentage of GNP in the composites.	92

Figure 4.16	Photodegradation activity of MB under UV-visible light irradiation for pure ZnO n.p and different weight percentage of GNP in the composites.	93
Figure 4.17	First-order Langmuir-Hinshelwood model of degradation kinetics study.	96
Figure 4.18	Influence of catalyst loading on MB degradation.	102
Figure 4.19	Influence of initial MB concentration on MB degradation.	104
Figure 4.20	Influence of pH solution for adsorption-desorption equilibrium.	106
Figure 4.21	Influence of pH solution for photocatalytic activity in MB degradation.	107
Figure 4.22	Influence of scavengers in the performance of pure ZnO n.p.	109
Figure 4.23	Influence of scavengers in the performance of 45% F-GNP/ZnO composite.	110
Figure 4.24	Proposed mechanism of 45% F-GNP/ZnO composite.	111

LIST OF ABBREVIATIONS

AOPs	Advance oxidation processes
BET	Brunauer-Emmett-Teller
BQ	Benzoquinone
CB	Conduction band
CO ₂	Carbon dioxide
FTIR	Fourier Transform Infrared Spectroscopy
HCl	Hydrochloric acid
H ₂ O	Water
HRTEM	High-Resolution Transmission Electron Microscopy
IPA	Isopropanol
L-H	Langmuir-Hinshelwood
MB	Methylene blue
MO	Methyl orange
MG	Malachite green
NaOH	Sodium hydroxide
NIR	Near-infrared
NH ₃	Ammonia

NO ₂	Nitrogen dioxide
PL	Photoluminescence
RhB	Rhodamine B
RR	Reactive red
SEM	Scanning Electron Microscopy
TEOA	Triethanolamine
THF	Tetrahydrofuran
TiO ₂	Titanium oxide
UV	Ultraviolet
UV-vis DRS	Ultraviolet-visible Diffuse Reflectance Spectroscopy
VB	Valence band
XRD	X-Ray Diffraction
ZnO	Zinc oxide

LIST OF SYMBOLS

		Unit
C	Concentration at time t	mg/L
C_0	Initial concentration	mg/L
E_g	Energy band gap	eV
e^{-1}	Electron	-
h^+	holes	-
H^+	Hydrogen ion	-
O_2^-	Superoxide radical	-
OH	Hydroxyl ion	-
OH	Hydroxyl radical	-
k_{ads}	Adsorption reaction rate constant	g/mg.min
k_{app}	Photocatalysis reaction rate constant	min ⁻¹
t	Reaction time	min
PZC	Point zero charge	-
R^2	Correlation coefficient	-
λ	wavelength	nm
θ	Bragg's angle in degree	-

**PRESTASI PEMFOTOPEMANGKINAN KOMPOSIT F-
GNP/ZnO DALAM PENYINGKIRAN METHYLENE BLUE DI BAWAH
PENYINARAN CAHAYA UV-VIS**

ABSTRAK

Krisis air buangan semakin bertambah buruk dan pengurangan pencemaran sepatutnya diambil serius untuk mengurangkan bahan cemar di dalam aliran air. Proses Pengoksidaan Lanjutan (AOP) dikenali sebagai salah satu cara yang efektif untuk mengatasi masalah dan pemfotomangkinan adalah pilihan yang terbaik di antara semua. Ini adalah kerana penggunaan tenaga boleh baharu menggunakan semikonduktor dan pada masa yang sama memineralkan bahan cemar yang berbahaya kepada produk tidak toksik iaitu CO₂ and H₂O. Novel komposit F-GNP/ZnO telah dihasilkan melalui “one-step solvothermal method”, di mana pengfusian oksigen GNP dan penghasilan komposit F-GNP/ZnO dilakukan serentak dalam satu masa. Oksigen-pengfusian kumpulan dengan jumlah yang rendah terlekat pada GNP telah ditunjukkan oleh spektroskopi Inframerah Transformasi Fourier (FTIR) dan berkolerasi dengan spektroskopi Raman. Pembentukan heterosimpang FGNP/ZnO telah ditunjukkan pada Pembelauan Sinar-X (XRD), Mikroskopi Elektron Pensakanan (SEM), Mikroskopi Penghantaran Elektron Beresolusi Tinggi (HRTEM), Tenaga Penyebaran Sinar-X (EDX), FTIR dan Brunauer-Emmett-Teller (BET) analisis yang membuktikan kontak rapat di antara F-GNP dan ZnO. Seterusnya, Kefotopendarcahayaan (PL) dan spektroskopi UV-visibel Kepantulan Baur (UV-vis DRS) telah berjaya membuktikan pengurangan penyatuan pasangan e^{-1}/h^{+} dan

penyerapan cahaya lebih luas berbanding ZnO tulen. Dalam kajian ini, aktiviti penyerapan dan pemfotomangkinan MB telah dilakukan dan mencapai komposit 45% F-GNP/ZnO sebagai optimum amaun GNP di dalam komposit dengan 70% kemampuan penyerapan dan 87% degradasi MB. Secara keseluruhan, 97% penyingkiran MB telah berjaya dilaksanakan dengan menggunakan komposit 45% FGNP/ZnO. Dengan itu, kemampuan penyerapan yang tinggi telah dibuktikan dengan menggunakan luas permukaan BET analisis, di mana luas permukaan berkadaran langsung mengikut amaun GNP di dalam komposit. FTIR dan Raman analisis juga telah menunjukkan satu keputusan bererti iaitu kehadiran interaksi $\pi - \pi$ di antara molekul MB dan F-GNP (rendah ketumpatan oksigen dalam struktur GNP) telah menyebabkan penyerapan MB molekul yang tinggi. Tambahan pula, kajian proses parameter merumuskan aktiviti pemfotomangkinan yang terbaik oleh komposit 45% F-GNP/ZnO telah dicapai menggunakan 0.1 g/L amaun pemangkin dalam 10 mg/L kepekatan MB pada pH 5. Selain itu, pseudo-tertib kedua bagi penyerapan dan pseudo-tertib pertama bagi aktiviti pemfotomangkinan untuk komposit 45% FGNP/ZnO telah didedahkan melalui kajian kinetik dan mendapat kadar 0.2250 g/mg.min and 0.034 min⁻¹, secara berturut-turut. Berdasarkan kajian pemerangkapan, radikal hidrosil telah dijumpai sebagai spesis paling aktif dalam degradasi molekul MB.

**PHOTOCATALYTIC PERFORMANCE OF F-GNP/ZnO COMPOSITE FOR
METHYLENE BLUE (MB) DEGRADATION UNDER UV-VIS LIGHT
IRRADIATION**

ABSTRACT

Wastewater crisis has been worsening and pollution abatement should be taken seriously to reduce the pollutant content in the water stream. Advanced oxidation processes (AOPs) is known to be an effective method to overcome this raised issue and photocatalysis is the best option among all. This is due to the utilization of renewable energy by using semiconductor and at the same time mineralized the harmful pollutant into non-toxic CO₂ and H₂O. A novel F-GNP/ZnO composites were synthesized via facile one-step solvothermal method, where the oxygen functionalization of GNP and F-GNP/ZnO composites formation were conducted simultaneously. The low-density oxygen-functional groups attached on GNP was shown by Fourier Transform Infrared Spectroscopy (FTIR) and correlated with Raman spectroscopy. The formation of F-GNP/ZnO heterojunction was shown in the X-Ray Diffraction (XRD), Scanning Electron Microscopy (SEM), High-Resolution Transmission Electron Microscopy (HRTEM), Energy Dispersive X-Ray (EDX), FTIR and Brunauer-Emmett-Teller (BET), that proves on the intimate contact between F-GNP and ZnO n.p. Then, Photoluminescence (PL) and UV-vis Diffuse Reflectance Spectroscopy (UV-vis DRS) has successfully provides the evidence on reducing recombination of electron-hole pairs and wider light absorption compared to ZnO n.p, respectively. In this study, adsorption and photocatalytic activity of MB was

studied and obtained 45% F-GNP/ZnO composite as the best GNP content in the composite with adsorption capability and degradation of MB up to 70% and 87%, respectively. In all, MB removal has successfully achieved with 97% by using 45% F-GNP/ZnO composite. Here, the high adsorption capability of the composites was proven by using Brunauer-Emmett-Teller (BET) surface area, where the surface area is directly proportional to the GNP content in the composites. FTIR and Raman analyses have shown a significant result, where the interaction that contributed to the high adsorption was $\pi - \pi$ interaction presence between MB molecule and F-GNP due to the low oxygen density in GNP structure. In addition, process parameter studies concluded that the best photocatalytic activity of 45% F-GNP/ZnO composite was achieved using 0.1 g/L catalyst loading in MB with concentration of 10 mg/L and pH 5. Moreover, pseudo-second order for adsorption and pseudo-first order for photocatalytic activity for 45% F-GNP/ZnO composite were revealed from kinetic studies and obtained rate of 0.2250 g/mg.min and 0.034 min⁻¹, respectively. Based on the scavenger test, hydroxyl radical was found to be the most active species that responsible for the degradation of MB.

CHAPTER 1

INTRODUCTION

This chapter gives an overview on wastewater issue and organic pollutant that causing it. Besides that, the conventional wastewater remediation and advanced oxidation processes are included. From that, a series of problem statements are listed, together with the research objectives to overcome the problems.

1.1 Wastewater Crisis

Water covers 71% of the earth surfaces, where the dominant contributions come from salt water and minorly from fresh water (Ahmed *et al.*, 2010). Generally, in the percentage of resources, water is an abundant resource and only the fresh water is utilized as it is neutral condition and does not require complicated process (Figure 1.1). However, fresh water is only 2.5% of the overall water percentage and most of it are trapped in the ice caps and glaciers, hence leaving at most 1% of fresh water that available to be used (Wecker, 2017). Thus, the usage of fresh water is extremely outnumbered due to its limited amount in the total coverage of water. In human and animal basic life, water plays an important role in transporting oxygen and blood throughout the whole body and digesting of food, where water is a medium for these mechanisms. For plants, water is needed for growth and transport of carbon dioxide, similar mechanism to animals and human being but different gases are transported (Rahman, 2016; Yaseen & Scholz, 2019). Aquatic life requires water the most, not only for growth and transporting gas medium, but for their habitat, in which their physical structure has been designed to live in water (Berradi *et al.*, 2019).

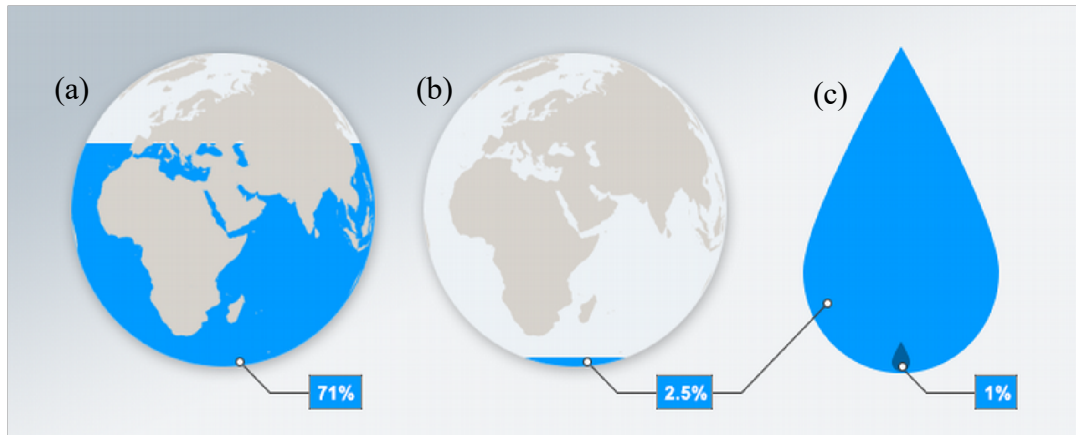


Figure 1.1: The percentage of (a) water in Earth resources, (b) fresh water among the Earth's water and (c) the available water to be used (Wecker, 2017).

Recently, fast-growing technology and industry have incurred a lot of pollutants in the environment, including water, air, land, noise and light pollution. Indicatively in Malaysia, among the various pollution, water is the most affected area as can be seen in Figure 1.2. Even though it is an abundant resource, due to the high usage from our daily life and wastes released into it, the demand of clear water supply has been increasing while the source of water supply remains constant (Krishnan *et al.*, 2017; Md Rosli *et al.*, 2018). Therefore, saving water and treating wastewater at our best is to save our planet and future mankind. Besides the basic life usage, the huge population and industries are worsening the water crisis at the expense of living and creating a better and easier life and in turn will cause high cost of environmental sustainability. A rapid industrial expansion especially petrochemical, pharmaceutical, textile, agricultural, food and chemical industry that produces waste effluent contaminated with organic compounds such as aromatics, haloaromatics and dyes have contributed to the contamination of fresh water in the ecosystem (Moussa *et al.*, 2016). The released of untreated organic pollutants are of high priority concern since they are harmful to the environment and carcinogenic to humans and animals even at low

contamination level in water at a few ppm concentration (Hadi *et al.*, 2015; Pang & Abdullah, 2013). Therefore, toxic and pollutant released into the aquatic environment is a major concern and proper remediation is considered as an urgent need.

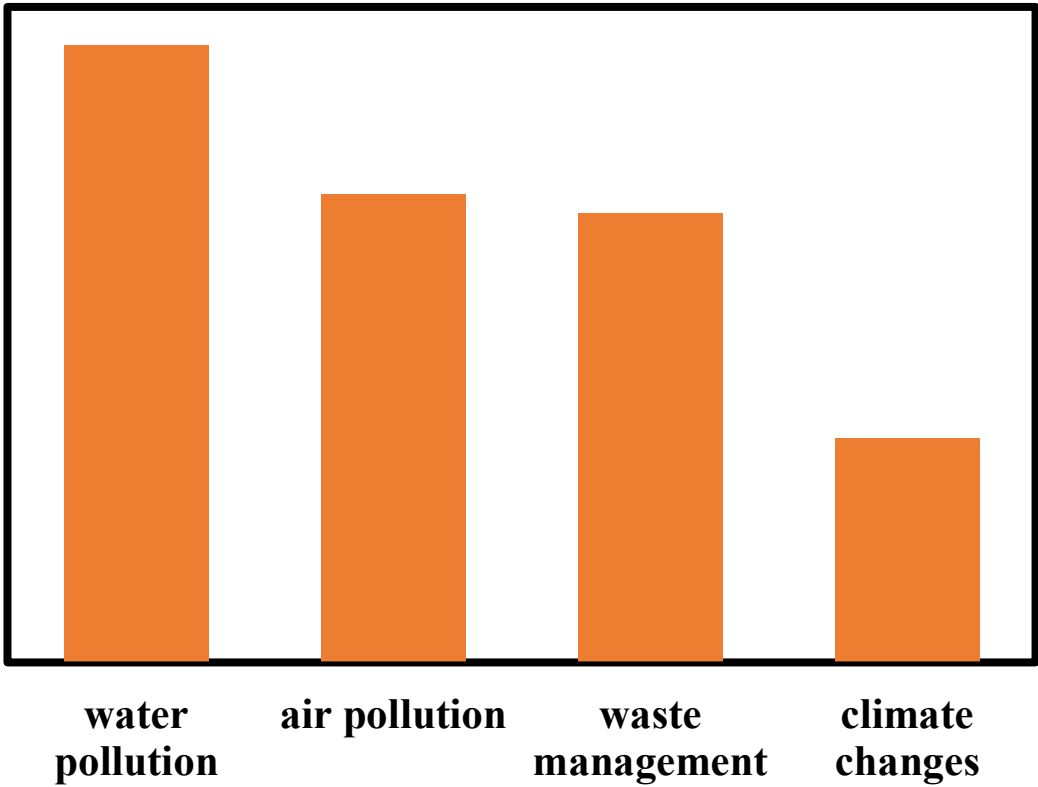


Figure 1.2: Statistical of different pollutions in Malaysia (Mei *et al.*, 2016).

1.2 Organic Pollutant

Specifically, textile industry has gradually increased in the world’s market since 2014 and is forecast to increase 5% globally in the year 2020 (Sivaram *et al.*, 2019). The Asia-Pacific region contributed 54.6% of the world textile industry (Lu, 2018). Malaysia categorically has huge number of textile industries in the east coast, thus organic pollutants produced could be the highest amount found in the wastewater effluent (Pang & Abdullah, 2013). The textile industry caused a waste of 280,000 tons of dyes per year and contain different type of dyes (Berradi *et al.*, 2019).

Basically, there are two types of classifications of synthetic dyes which are based on their (1) chemical structure and (2) application on different substrates. For the first classifications, Table 1.1 categorizes the dyes by chromophoric groups and begin with azo dyes that constitute 70% of the world's annual production of synthetic dye (Nakkeeran *et al.*, 2018). Azo dyes are characterized with the presence of azo groups (-N=N-) linked to the -OH or -NH₂ groups. Nitro and nitroso dyes are characterized by the presence of a nitro group (-NO₂), while anthraquinone dyes consists of hydroxyl or amino groups. On the other hand, phthalocyanine dyes are dye with the presence of a metal type such as Cu, Ni, Co and Pt (Osman *et al.*, 2017). The second classifications are tabulated in Table 1.2 that categorizes the dyes based on the field applications. This classification is made based on the solubility in water solvent, thus there are two categories of dyes: water-soluble and water-insoluble dyes. The well-known type of dyes are in the water-soluble dyes category that have anionic, cationic, metalliferous and reactive dyes which consists of azo, anthraquinone and phthalocyanine chromophoric groups (Nanakkal & Alexander, 2017). Whereas the insoluble dyes did not possess any of the chromophoric groups, because these dyes are mostly applied in the finishing process in order to tighten and lock the dyes in the fabric (Nakkeeran *et al.*, 2018). Besides that, azo dyes are one of the organic pollutants which is carcinogenic to humans and animals.

Table 1.1: Classification of dyes based on the chromophores and auxochromes groups
(Berradi *et al.*, 2019).

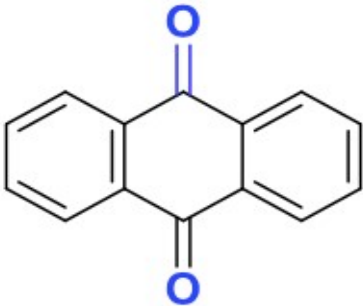
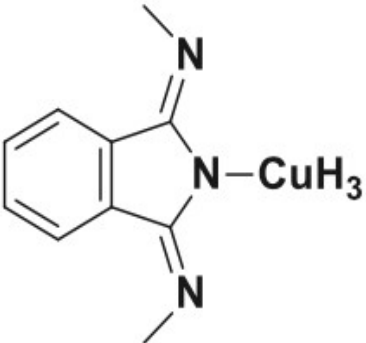
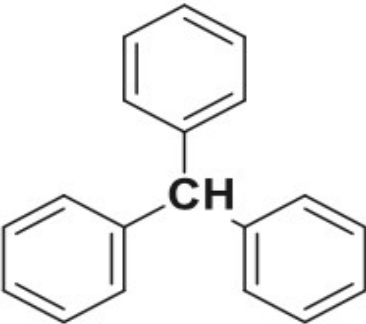
Type of dye	Chromophore group	Auxochrome group
Azo	(-N=N-)	Amino (-NH ₂)
Nitroso	(-NO or -N-OH)	Methylamino (-NHCH ₃)
Nitro	(-NO ₂ or =NO-OH)	Alkoxy (-OR)
Anthraquinone		(-OCH ₃) Cl, Br, I, At
		
Phtalocyanine		
		
Triphenylmethane		
		

Table 1.2: Classification of dyes based on the auxochromes groups (Rahman, 2016).

Solubility	Type of dyes	Chromophores or structure	Example
Water-soluble dyes	Acid/anionic dyes	Azo, anthraquinone	Acid blue 74, acid blue 90, red acid 27 (AR27)
	Basic/cationic dyes	Azo, anthraquinone	Methylene blue (MB), basic blue 9 (BB9), basic yellow 37 (BY37)
	Metalliferous dyes	Azo, phthalocyanine	Pigment blue 15/3, Nickel (II) tetrasulfonic acid, iron (III) phthalocyanine chloride
	Reactive dyes	Azo, anthraquinone, phthalocyanine	Reactive red 198 (RR 198), red cibacrom 3 (RC3)
Insoluble dyes	Pigments	Not contain any group	Benzoic derivatives and inorganic pigments derived from metals.
	Disperse/dispersible dyes	Anthraquinone	Red disperse 60 (RD60) and blue disperse 7 (BD7)
	Fixing different dye classes	Not contain any group	-

In addition to that, wastewaters containing organic pollutants have severe impacts towards aquatic life, human beings and animals. Firstly, the discharged wastewater effluent by textile industries in rivers and oceans has a great effect to the aquatic flora and fauna. The presence of dyes in the water stream and oceans has

prevented light penetration, hence reducing the photosynthesis of aquatic fauna (Chong *et al.*, 2010; Grandclément *et al.*, 2017). While the aquatic flora suffered with the changing environmental conditions due to the hazardous dyes. On top of that, human beings could have faced with several dangerous health problems such as allergies, dermatitis, skin irritations, cancers and mutations (Grandclément *et al.*, 2017). Around 60 to 70% of azo dyes are highly toxic and carcinogenic due to their resistance to conventional physicochemical destruction and the absence of biodegradability (Nakkeeran *et al.*, 2018). It has been reported the most toxic dyes are found in the azo dyes and specifically, diazo and cationic dyes. The most commonly used in textile industries are the azo dyes such as Methylene Blue (MB), Methyl Orange (MO), Rhodamine B (RhB) and Reactive Black 5 (RB 5) (He *et al.*, 2011; Yaseen & Scholz, 2019). The aforementioned dyes are actively used in dyeing clothes and removing excess dyes on the clothes will then cause persisting dye molecules in the water. It has been well known that MB is a recalcitrant dye solvent due to its deep blue colour. Therefore, even though the concentration of MB dye is only 10 ppm, but the purification and treatment process will still be complicated (Pang & Abdullah, 2013). The treatment for this wastewater effluent will not only require high cost, but also a large area and longer period.

1.3 Conventional Wastewater Remediation

Numerous technology and treatment of wastewater effluent have been reported from the previous years in the literature. It can be divided into three categories: physical, chemical and biological methods. These methods have their own benefits and drawbacks, not only to the water itself, but in the worst case scenario, it can affect the other resources such as air and land (Krishnan *et al.*, 2017). For the physical method, the adsorption and membrane filtration were found to be the dominant process for

wastewater remediation (Yaseen *et al.*, 2019). The physical method is known to be the easiest way to decontaminate the water, but it has limited lifetime and constant replacement is needed as it will introduce fouling after it reaches a saturation point (Berradi *et al.*, 2019). The chemical method as its name, requires huge amount chemicals during the process and consequently produce second pollution which is sludge. The example of the most effective chemical method is chlorination and ozonation (Rahman, 2016). On the other hand, biological method is starting to get the attention from the researchers due to the usage of bio-life and many studies have been carried out to investigate the effectiveness in the wastewater remediation (Grandclément *et al.*, 2017; Gulyas *et al.*, 2013; Mei *et al.*, 2016). Most of these studies reported on high performance of biological method, however, it requires large area, longer time and expensive procedure (Gulyas *et al.*, 2013). To be noted, each of these conventional methods still require physical method usually in the final process, where most employ the facile filtration process to recover the adsorbent, chemicals catalyst or biological materials (Grandclément *et al.*, 2017).

1.4 Advance Oxidation Processes (AOPs)

Advanced oxidation processes (AOPs) are processes producing reactive hydroxyl radicals species ($\bullet\text{OH}$), where it is unselective in degradation activities. In order to achieve high number of hydroxyl radicals species, the primary oxidant is needed such as ozone, hydrogen peroxide and oxygen and/or energy sources or catalysts (Fujishima & Honda, 1972; Nakkeeran *et al.*, 2018). AOPs have been known as a promising method in degradation of organic pollutant. The AOPs count on the oxidation of toxic materials through production of hydroxyl radical species ($\bullet\text{OH}$). At the same time, generation of other species was taken into account for the formation of

hydroxyl radicals as it can be one of the reasons in higher mineralization of contaminants. Mostly, AOPs were employed towards secondary treatment effluent and called as tertiary treatment (Pang & Abdullah, 2013). Thus, the process will mineralize hazardous organic pollutant into non-hazardous compounds such as water, carbon dioxide and salts. It is well-known that the AOPs are employed in the Fenton process, ozonation, photolysis and photocatalysis, whereby photocatalysis requires semiconductor with high reduction or oxidation potentials and light energy (Krishnan *et al.*, 2019). Furthermore, the effectiveness of photocatalysis was reported with pollution abatement from several hundred ppm to less than 5 ppb (Chong *et al.*, 2010). Compared to other AOPs, photodegradation of organic pollutant is found to be more reasonable and practical due to the conversion of organic pollutant into non-toxic wastes and no secondary pollution is produced (Meng *et al.*, 2016).

1.5 Semiconductor Photocatalysts

Photocatalysis has captivated great attention starting from the investigations of water splitting by Fujishima and Honda's by utilizing photocatalyst and solar energy (Fujishima & Honda, 1972). The photocatalyst employed was a semiconductor that has electronic band gap properties, comprising of valence band maximum (VB) and conduction band minimum (CB). The occupied electrons was stated at VB, while the unoccupied electrons was stated at CB therefore the band gap energy of semiconductor can be calculated (Shafawi *et al.*, 2020; Sin *et al.*, 2013). The tremendous properties of semiconductor makes it sensitized under light irradiation, following the wavelength of light absorbed by the semiconductor that corresponds to the band gap energy of semiconductor. In addition, higher gap energy of semiconductor (> 3.0 eV) can only be photoactivated under UV range (< 380 nm) of light that only makes up 5% from solar energy, whereas semiconductor with energy gap of 1.6 eV to 3.2 eV has the

ability to absorb more wavelength of light which is in the visible light range (380 – 740 nm) that comprises 40% of the solar energy (Md Rosli *et al.*, 2018). The commonly used photocatalysts are TiO₂, ZnO, CdS and etc., when under light illumination will excite electrons from VB to CB that has the potential to reduce and oxidize oxygen and water molecules, respectively. Then, the produced radicals' species will produce hydroxyl radicals which in turn degrade the contaminants into harmless compounds.

1.6 Problem Statement

As one of the low-cost technologies in the field of environmental protection, tremendous developments in both the theories and experiments of photocatalysis have been achieved because of the worsening pollution problem (Tang *et al.*, 2018). Among the semiconductor photocatalysts, TiO₂ and ZnO have extensively been investigated until now because of low toxicity, high stability and low cost. It is reported that ZnO shows better efficiency than TiO₂ for the degradation of some organic dyes during photocatalytic process (Nanakkal & Alexander, 2017). Furthermore, ZnO has comparable band gap energy with TiO₂, have high exciton binding energy (60 meV) and it offers advantages in certain organic pollutant degradation compared to TiO₂ (Ghule *et al.*, 2011). However, the usage of ZnO in photoactivity has high recombination ratio of photoinduced electron-hole pairs and very poor response to visible light because of its wide band gap (3.2 eV), which absorbs UV light with wavelengths below 387 nm (Liu *et al.*, 2012; Zhang *et al.*, 2019). Besides that, one of the major challenges of ZnO semiconductor is to improve the photoinstability due to the photocorrosion in the presence of light irradiation which decreases the photocatalytic activity. Thus, many modifications have been done to improve the photocatalytic activity of ZnO like surface morphology changes of ZnO or surface modifications by non-metal doping, addition of transition metal as well as coupling

with other semiconductors (Atchudan *et al.*, 2016; Moussa *et al.*, 2016; Yayapao *et al.*, 2013; Zhao *et al.*, 2017; Zhou *et al.*, 2012).

Recently, numerous researches have carried out semiconductor coupling or known as heterostructure photocatalyst. To date, graphene has been proposed as one of the rising materials in photocatalysis, but graphene alone is a weak photocatalyst. In fact, pure graphene flakes was hardly found in photocatalytic work due to its hydrophobic properties and unsuitable for direct use in water splitting (Yeh *et al.*, 2013). Based on the theoretical findings, it has been proven that graphene has metallic properties where its half-filled electron band touches the fermi level producing gapless energy (Geng *et al.*, 2013). This metallic property is somehow advantages in accepting electron from semiconductor under light illumination, thus heterojunction of graphene with other semiconductors could enhance the photocatalytic process. Graphene has great properties in the adsorption capability because of its high surface area and its high electron mobility relatively prevented recombination of charge carriers gives an efficient photodegradation (Liu *et al.*, 2013; Lonkar & Abdala, 2014). Previous studies have shown that forming heterojunction between graphene and other semiconductors such as TiO₂, ZnO, ZnS and CdS have improved the photoactivity (Ahmad *et al.*, 2013; Chen *et al.*, 2013; Nanakkal & Alexander, 2017). This is because of the high electron mobility of graphene that is beneficial for providing a greater number of surface active sites for photocatalytic reactions which was attributed to the rapid separation of charge carriers across graphene and semiconductors heterojunction (He *et al.*, 2011; Wang *et al.*, 2017).

On the other hand, there are many methods to synthesize graphene and ZnO nanoparticles that will affect oxygen-functional group attached on graphene. One of the common method used to functionalize the graphene is by acid treatment using sulphuric acid, nitric acid and hydrochloric acid (Firdaus *et al.*, 2019; Wang *et al.*,

2015). The acid treatment used to add oxygen-functional group in the graphene structure was a great idea but will result in higher band gap energy which does not improve light harvesting. Therefore in this study, the one-step solvothermal process using THF has been proposed to control the oxidation level of graphene, in order to produce smaller bandgap energy and at the same time, form composites with ZnO particles. To the best of our knowledge, one-step solvothermal process producing functionalized graphene with zinc oxide (F-GNP/ZnO) was scarcely reported and further research can be done to study the improvement of physisorption ability of FGNP/ZnO composite photocatalyst and the enhancement of the electron transport at the interphase between GNP and ZnO.

1.7 Research Objectives

The aim of this research is to develop a photocatalyst with high photocatalytic activity to degrade MB dye under UV-vis light irradiation. The specific objectives of this research are:

1. To prepare the F-GNP/ZnO composites by one-step solvothermal method and characterize physical and chemical properties of F-GNP/ZnO composites.
2. To investigate the effect of mass ratio of F-GNP/ZnO composites with different amount of GNP on the adsorption and photodegradation performances.
3. To evaluate the effect of process parameter on photocatalytic degradation of MB dye: catalyst loading, initial concentration of MB dye and pH solution.
4. To identify the kinetic process of adsorption and photodegradation under optimum weight percentage of GNP.

1.8 Scope of Study

The purpose of this study is to modify ZnO semiconductor by forming heterostructure photocatalyst with Functionalized Graphene Nanoplatelets (F-GNP) to produce UV-vis light sensitized photocatalyst. The functionalization of GNP and composites formation was carried out in a one-step solvothermal method. The facile synthesizing method was chosen because it will produce low density oxygen functional group on GNP structures, therefore will yield F-GNP which possess low defect density. The sample produced was characterized by using X-Ray Diffraction (XRD), Scanning Electron Microscopy (SEM), Elemental Dispersive X-Ray (EDX), High-Resolution Transmission Electron Microscopy (HRTEM), Fourier Transform Infrared spectroscopy (FTIR), Raman spectroscopy, surface characterization analyzer, zeta-potential, Ultraviolet-visible Diffuse Reflectance Spectroscopy (UV-vis DRS) and Photoluminescence (PL) spectroscopy. The weight percentage of GNP in the composites were varied from 15%, 30%, 45% and 60%. The F-GNP/ZnO composites were studied for their adsorption and photocatalytic activities to obtain the best composite with high performance for both mechanisms. In the latter case, the best composite was investigated under few operating parameters: effect of catalyst loading, effect of MB initial concentration and pH of dye solution towards MB removal. Here, the optimum conditions for the F-GNP/ZnO composite can be determined. Subsequently, since the GNP content in the F-GNP/ZnO composites affected the adsorption activity, therefore the adsorption kinetic study was analyzed. Similarly, MB degradation kinetic model was investigated for different GNP content in the composites. Finally, pseudo-second order and pseudo-first order for adsorption and photocatalytic activity were revealed in this study, respectively. In order to prove the MB degradation occurs during the reaction and to identify the major reactive species

that largely responsible to attack MB molecule, scavenger test was investigated for pure ZnO and the best composite.

1.9 Thesis Organization

This thesis consists of five chapters. Chapter 1 (Introduction) relates to the current issue and description on photocatalytic activity. It also contains a brief explanation on the modification of ZnO semiconductor for higher wavelength of light absorption and higher MB degradation. Besides that, graphene as carbon-based electron acceptor for ZnO photocatalyst was introduced. The problem statements in this research area were discussed thoroughly and subsequently, the objectives and scope of study were explained.

Chapter 2 (Literature Review) contains description on the background of this research study regarding carbon-based material, ZnO semiconductor and their application in photocatalytic activity. This chapter begins with the properties of MB, details on photocatalysis, modification of ZnO semiconductor and catalyst preparation.

Chapter 3 (Materials and Methods) describes the materials and chemicals used and their properties. The details on methodology on catalyst preparation, experimental section and catalyst characterization are explained and illustrated in this chapter. It also includes the process parameter studies and kinetic studies for both adsorption and degradation activities.

Chapter 4 (Results and Discussion) shows the findings from this research work. In this chapter, each of the characterizations were explained and compared with previous studies. After that, it discusses on the adsorption and degradation activities, including the kinetic studies for both activities. The scavenger test and photocatalytic mechanism were provided in this chapter in order to prove the MB degradation.

Chapter 5 (Conclusions and Recommendations) summarizes the conclusions from the results obtained in this research work. The future recommendation is presented in this chapter.

CHAPTER 2

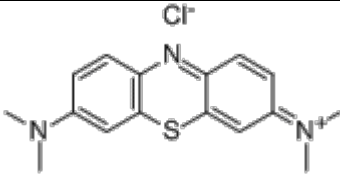
LITERATURE REVIEW

In this chapter, the review were made on organic pollutant specifically MB that was abundantly found in wastewater effluent in textile industry and photocatalysis as pollutant abatement by employing ZnO as photocatalyst. Summary of graphene as support in photocatalysis were sufficiently described, together with the synthesizing method.

2.1. Properties and Application of MB

MB is a one of azo dyes, widely being used in dyeing textile fibers. They are considered to be easy to use, relatively cheap and provide clear, strong colours (Chong *et al.*, 2010; Meng *et al.*, 2016). MB anhydrous is a compound consisting of dark green crystals or crystalline powder, having a bronze-like cluster. When MB is diluted in water or alcohol, it has a deep blue colour. In fact, MB is a synthetic basic dye and stains to negatively charged cell. It is being used in textile industries, such as cotton, silk, wool, leather and mordant with the tannin dyeing process as well as ink and copying paper (Huang *et al.*, 2013). Previously, it has been used for printing of cellulose acetate and unspectacularly, become a need in textile dyeing process in part of the development synthetic fibers such as polyacrylonitrile, acid-modified polyester and polyamide fibers (Nakkeeran *et al.*, 2018). Table 2.1 summarizes the basic chemical properties of MB.

Table 2.1: Properties of MB (Hadi *et al.*, 2015; Qiao *et al.*, 2016).

Structural formula	
Empirical formula	C ₁₆ H ₁₈ ClN ₃ S
Molecular weight (g/mol)	319.85
Boiling point (°C)	190
Water solubility (r.t)	40 g _{MB} /1000 mL _{H₂O}
Flash point	45

2.2. Photocatalysis

It was first found in 1911 by a German scientist, Dr. Alexander in decolourization of dark blue pigment by ZnO under light illumination (Eibner, 1911). Later, an article was published in disintegration of oxalic acid by uranic salt under light irradiation (Bruner & Kozak, 1911). This process occurs at the ambient temperature and pressure that is beneficial for the wastewater treatment because it will make the process practical. There are five main steps in photocatalytic reaction in semiconductors including (Low *et al.*, 2017):

- i) Light absorption by the semiconductor.
- ii) Formation of photogenerated electron-hole pairs.
- iii) Migration and recombination of the photogenerated electron-hole pairs.
- iv) Adsorption of reactants and desorption of products.
- v) Occurrence of redox reactions on the semiconductor surface.

Photocatalysis process requires light irradiation in the presence of semiconductor to accelerate the remediation of organic contaminants. The

photocatalyst employing semiconductor such as TiO₂, ZnO, Fe₂O₃, GaP and ZnS has demonstrated a non-toxic properties and produce non-harmful carbon dioxide gas and water molecule (Belver *et al.*, 2019). Firstly, a semiconductor has the ability in absorbing light with a condition that the photon is similar or higher energy than its gap energy. Here, the band gap energy of semiconductor can be defined as follows:

$$E_g = VB - CB \quad \text{Eq. (2.1)}$$

where E_g represents band gap energy (eV), VB represents highest occupied molecular orbital (HOMO) and CB represents lowest unoccupied molecular orbital (LUMO). Secondly, the photon absorbed by the semiconductor induced excitation of electron from VB to CB, hence leaving holes in the VB. Figure 2.1 illustrates the schematic diagram of photogenerated electron-hole pairs in semiconductor.

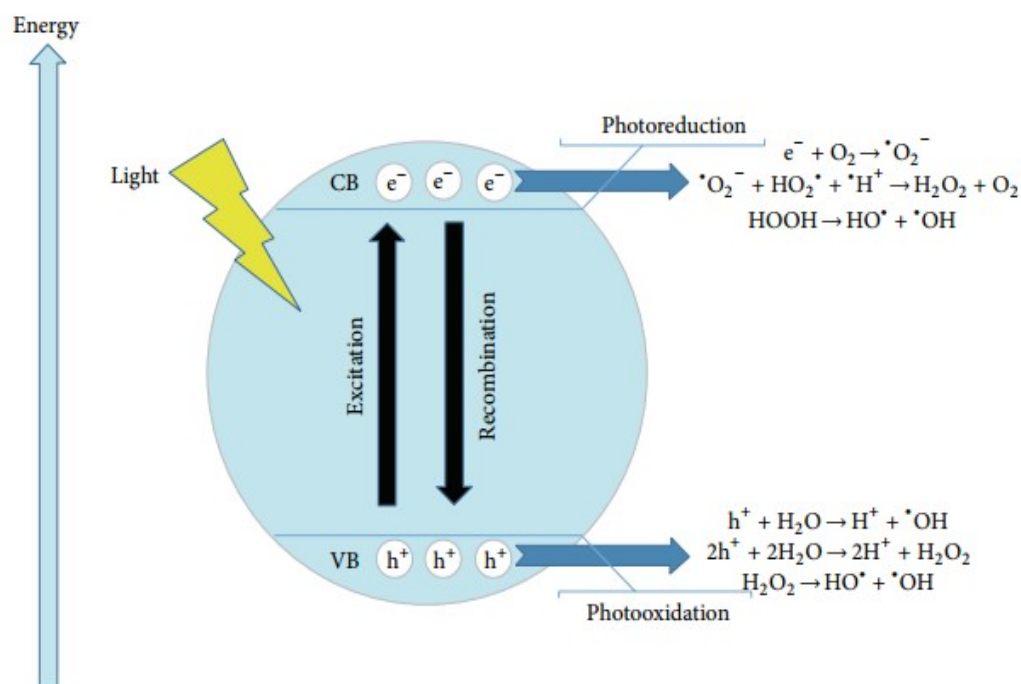
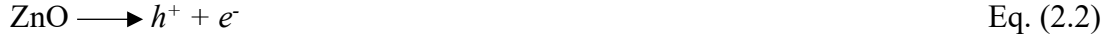


Figure 2.1: Schematic diagram of heterogeneous catalyst mechanism (Moniz *et al.*, 2015).

When the catalyst absorb higher energy than its band gap energy, it will lead to the formation of positive hole (h^+) in the VB and excitation of electron to the CB. The electron promoted from VB to CB, results in electron-hole pairs.



Thirdly, the photogenerated electron reduces the oxygen adsorbed on the catalyst to superoxide radical anions ($\cdot\text{O}_2^-$). The $\cdot\text{O}_2^-$ will then undergo a series of reaction to form $\cdot\text{OH}$ radicals. Eq. (2.3) - (2.6) illustrates the reaction (Qiao *et al.*, 2016).



The photogenerated holes oxidize water or hydroxyl ions (OH^-) to form hydroxyl radical ($\cdot\text{OH}$) as shown in Eq. (2.7) - (2.8) (Sin *et al.*, 2013).



However, there are two possibilities path that could occur in this step, where (a) the photogenerated electron at CB recombined with holes at VB, and (b) photogenerated electron migrated to another semiconductor. Path (a) gives disadvantage in the photocatalysis activity, while path (b) benefits in mineralization of organic pollutant in which photogenerated electron and holes will then reduce O_2 and oxidize H_2O molecules, respectively (Hu *et al.*, 2013). Semiconductor catalysts faced a significant problem in photocatalytic area which is its recombination of

photogenerated electron-hole pairs. This issue can possibly occur in the volume of catalyst or surface of catalyst, with the release of heat and light as by-product (Dominguez *et al.*, 2014; Umar & Aziz, 2013).

Fourth, the adsorption-desorption reactants occurred on the surface of photocatalyst until it achieved equilibrium. Lastly, redox reactions by the photogenerated electron-hole pairs produced reactive $\cdot\text{OH}$ radicals, then the complete mineralization of organic pollutant into CO_2 and H_2O molecules by the radicals (Moussa *et al.*, 2016). The hydroxyl radicals ($\cdot\text{OH}$), holes (h^+) and superoxide radical anions ($\text{O}_2^{\cdot-}$) has been proven as the highly reactive oxidizing species that will oxidize organic pollutant into harmless product, CO_2 and water (Tang *et al.*, 2018).

There are several advantages of heterostructure photocatalyst offers, such as photocatalytic activity can occur at ambient conditions, provides complete mineralization of organic pollutant into CO_2 and the formation of photocatalyzed intermediate stable product is avoided (Merabet *et al.*, 2009). Besides that, the oxidant molecules produced during this process, were found to be safe and very efficient for the mineralization of organic pollutant (Ramachandran & Sivasamy, 2019). There are few studies reported that the other oxidant species were also involved, but it was found that hydroxyl radical was the dominant species produced during the purification process (Sinha *et al.*, 2019; Umar & Aziz, 2013). Therefore, hydroxyl radical species has been denoted as a very reactive species that are continuously produced along the photochemical reaction. By utilizing semiconductor such as TiO_2 (Fujishima & Honda, 1972; Lam *et al.*, 2010), ZnO (Jyoti *et al.*, 2013; Rosli *et al.*, 2015; Sin *et al.*, 2013), $g\text{-C}_3\text{N}_4$ (Huang *et al.*, 2013; Md Rosli *et al.*, 2018; Shafawi *et al.*, 2020) and etc., under solar light, it will excite electron thus continuously producing hydroxyl radical species through reduction of dissolved oxygen in organic pollutant solution. On the other hand,

the holes generated at the VB are also participating in the oxidation of water molecules into hydroxyl radicals. Therefore, both electron and holes are important to generate hydroxyl radicals for decontamination of organic pollutant.

By utilizing photocatalysis, the mineralization of organic pollutants can be achieved efficiently in which the final products are carbon dioxide gas (CO₂) and water (H₂O) molecule (Xu *et al.*, 2018). Besides that, by employing photocatalysis, it does not require any expensive oxidant because oxygen is used as chemical oxidant and the used photocatalyst are also self-regenerated, where it can be reused and recycled without harsh and vigorous treatment (Shafawi *et al.*, 2020). The photocatalysis employed of chemical oxidants to remove both COD and BOD materials and organic pollutants in the wastewater effluent. The process is mainly driven by the mechanism of intermediate reactive hydroxyl radicals ($\cdot\text{OH}$) in aqueous phase (Barzgari *et al.*, 2016). Table 2.2 lists the comparative oxidizing power for different oxidants.

Table 2.2: Comparative oxidizing power of different oxidants (Teoh *et al.*, 2012).

Oxidants	Oxidizing potential (eV)
Hydroxyl radical ($\cdot\text{OH}$)	2.80
Sulphate radical ($\cdot\text{SO}_4^-$)	2.60
Ozone (O ₃)	2.07
Persulphate (S ₂ O ₈)	2.10
Hydrogen peroxide (H ₂ O ₂)	1.80
Perhydroxyl radical ($\cdot\text{HO}_2$)	1.70
Permanganate ion ((Mn) ₄)	1.70
Superoxide radicals ($\cdot\text{O}_2$)	-2.40

In recent years, heterostructured photocatalysts have attracted attention in research because of its powerful potential applications in solving many energy and

environment challenges at global levels in economically sustainable manner (Li *et al.*, 2016). The reason on researcher focusing in the heterostructured photocatalyst is because single semiconductor that work as a photocatalyst will result on high recombination of electron-hole pairs. Among other methods to separate the photogenerated electron-hole pairs of semiconductor such as doping and metal loading, forming heterostructured photocatalyst is a promising ways because of its feasibility and effectiveness for spatial separation of electron hole pairs (Low *et al.*, 2017).

2.3 ZnO in Photocatalysis Process

ZnO has been classified as a safe material by Food and Drug US (FDA), even though, it is an acidic compound (Jyoti *et al.*, 2013). Table 2.3 summarizes the properties of ZnO.

Table 2.3: Properties of ZnO semiconductor (Henni *et al.*, 2019; Peter *et al.*, 2018).

Physical properties	White colored powder
Molar mass	81.38 g/mol
Solubility	Soluble in water, acid and alkali
Crystal structure	Wurtzite, rocksalt and zinc blende
Band gap energy, E_g (eV)	~ 3.2 eV (VB = 2.7, CB = -0.5)

The physical properties of ZnO is white-colored powder, nearly soluble in water but soluble in acids and alkalis (Md Rosli *et al.*, 2018). ZnO can be found in three different structures such as wurtzite, zincblende and rocksalt as shown in Figure 2.2. The most commonly found structure is wurtzite ZnO as it is thermodynamically

stable structure, hence tremendous amount of photocatalysis studies are focused in this structure. Rahman *et al.*, reported that ZnO is a polar crystal where the O^{2-} are hexagonal packed and Zn^{2+} lies between the tetrahedral hole of four O^{2-} ions (Rahman *et al.*, 2013). On the other hand, rock salt structure can be obtained at relatively high pressure, while zinc blende structure may be stabilized only by the growth on cubic substrates (Morkoç & Özgür, 2008).

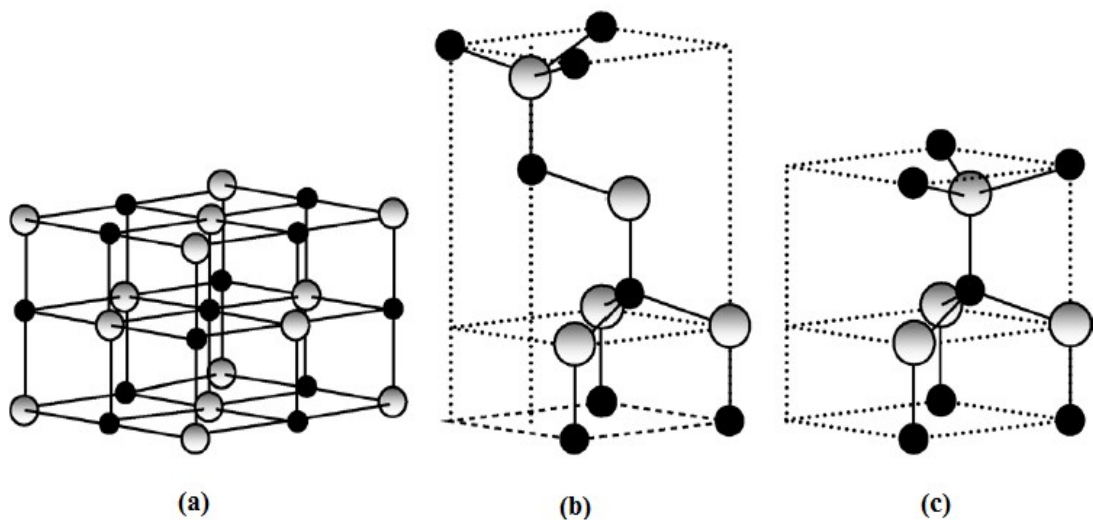


Figure 2.2: Crystal structure of ZnO (a) cubic rocksalt, (b) cubic zinc blende and (c) hexagonal wurtzite ZnO. Shaded grey and black circles denoted as Zn and O atoms, respectively (Morkoç & Özgür, 2008).

In photocatalysis, semiconductors like ZnO, TiO_2 and Fe_2O_3 act as sensitizers for light-induced redox-processes. This is because of the electronic structure of the metal atoms in chemical combination, which is characterized by a filled VB, and an empty CB (Regmi *et al.*, 2018). Figure 2.3 illustrates the band gap energy for different semiconductors.

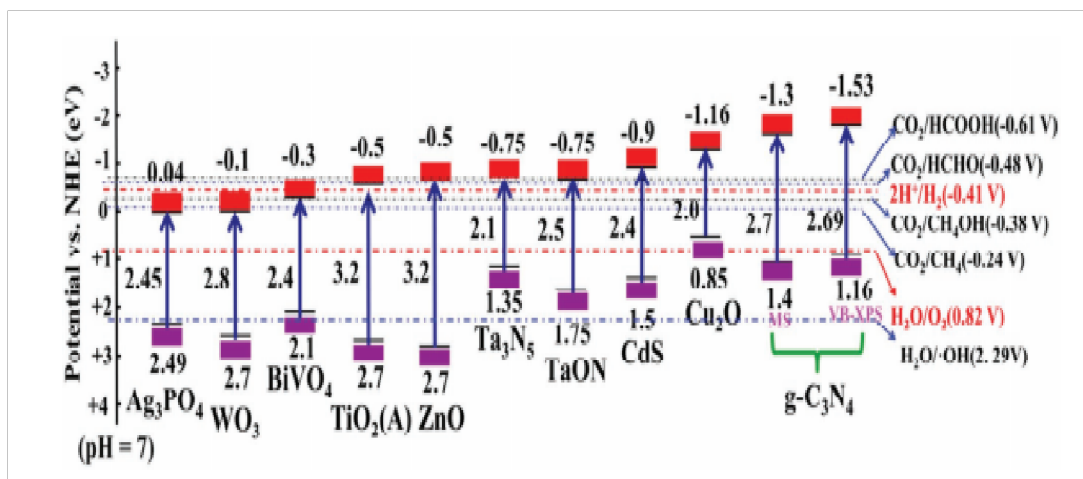


Figure 2.3 : Band gap position of different semiconductors (Ma *et al.*, 2017).

As can be seen in Figure 2.3, the band gap of semiconductors obtained are responsible in the light absorption, whether the semiconductor is sensitized under UV or visible light irradiation (Sinhamahapatra *et al.*, 2015). For photocatalysis reaction to occur, recombination of the electron and hole pairs must be prevented as much as possible. This is because recombination of electron and hole pairs may result in low quantum yields for most photocatalytic reaction (Liu *et al.*, 2012). Due to this problem, heterostructured photocatalyst is one of the methods suggested to inhibit the recombination and enhance the activity.

In reduction-oxidation potential, ZnO possessed a high oxidizing potential with VB value of 2.7 eV, and a reducing potential with CB value of -0.5 eV (Weiss *et al.*, 2019). This high oxidizing potential is beneficial in oxidizing dissolved oxygen molecule into hydroxyl radicals that are responsible to mineralize organic molecules. Even though the reducing potential is quite low but the value is more negative than the redox potential of dissolved oxygen (0.82 eV), therefore the reduction of oxygen molecule can still occur to produce superoxide radical which further reduces the water molecule to form hydroxyl radical (Samad *et al.*, 2016).